Desalination and Water Treatment
www.deswater.com

doi: 10.1080/19443994.2013.826786

52 (2014) 775–783
January

Taylor & Francis
Taylor & Francis Group

Removal of phosphate from water using raw and activated laterite: batch and column studies

Ling Zhang[a], Wentao Wu[a], Jianyong Liu[a,*], Qi Zhou[a], Jinghuan Luo[a], Jianqiu Zhang[a], Xinze Wang[b]

[a]*School of Environmental and Chemical Engineering, Shanghai University, 333 Nanchen Road, Shanghai 200444, China*
Tel. +86 21 6613 7748; Fax: +86 21 6613 7761; email: liujianyong@shu.edu.cn
[b]*School of Environmental Science and Engineering, Shanghai Jiaotong University, 800 Dongchuan Road, Shanghai 200240, China*

Received 23 March 2013; Accepted 5 May 2013

ABSTRACT

This paper describes the removal of phosphate from wastewater using raw laterite (RL) and activated laterite (AL) according to batch and column adsorption experiments. Single factor experiment was performed to identify the optimal activation conditions. The results showed that sample prepared by heating the laterite at 700℃ for 2 h (AL) had the optimal performance. The effect of various factors such as pH, dosage, and coexisting ions on the performance of the two kinds of laterite was investigated. The activated materials exhibited higher phosphate removal over broader pH range compared with the raw ones. Langmuir model fitted the isotherm adsorption data well and the maximum adsorption capacities of the RL and AL were calculated to be 0.90 and 1.86 mg/g, respectively. Pseudo-second-order model fitted the kinetics data well, indicating that the adsorption was mainly related to chemical adsorption. Column experiments were carried out with constant influent concentration and bed depth and various initial phosphorus concentrations to evaluate the practical application of laterite to the continuous removal phosphate from water.

Keywords: Phosphate removal; Raw laterite (RL); Heat-activated; Activated laterite (AL); Column adsorption

1. Introduction

The presence of excess phosphate in wastewater is one of the main causes of eutrophication that affects many natural water bodies [1,2]. Therefore, phosphate removal in the domestic and industrial effluent is absolutely necessary in order to avoid eutrophication. Phosphate removal from water can be achieved by several methods, mainly including biological removal [3,4], chemical precipitation by ferric or aluminum salts [5,6], ion exchange [7], and adsorption [8,9]. Using biological method with low cost, the wastewater quality can hardly meet the discharge criterion, which means that the remaining phosphate

---

*Corresponding author.

Presented at the Fifth Annual International Conference on "Challenges in Environmental Science & Engineering—CESE 2012" Melbourne, Australia, 9–13 September 2012

should be removed by other way [10–12]. Chemical method is widely accepted, such as lime, alum, and ferric chloride are the common precipitants used for phosphate removal [13]. But their cost and sludge productions make chemical treatment an unattractive option for wastewater treatments [14].

Adsorption seems to be attractive for the phosphate removal due to its simplicity of operation, low cost, phosphate removal steadily, and the possibility of phosphate recovery [9]. In recent years, considerable attention has been paid based on economic and environmental concerns to the study of using different types of low-cost sorbents such as alum sludge [15], red mud [16,17], fly ash [18], and other waste materials [19,20] as alternative adsorbents for sorption of phosphate from water. Nevertheless, the sorbent with low cost and large sorption capacity should be selected to satisfy both economic efficiency and convenience.

Laterite, a red brown soil with rich Fe–Al-oxide, presents widely in the subtropical hilly region mostly between latitude 25–31° with total area of 56.9 million ha in China. Because of its high content of active constituents such as aluminum, iron, and calcium, laterite has been found to remove fluoride [21], arsenate [22], Cu^{2+}, Zn^{2+}, Ni^{2+}, Cd^{2+}, and Cr^{6+} [23–25] from aqueous solution, and remove phosphate [26–29] in the seawater as well. So, laterite, with sufficiency and low cost, should be considered as a viable alternative to competitive adsorbent for phosphate removal in these areas.

Although the laterite was found to be a good adsorbent for phosphate removal [30], the direct use of laterite without activation is not appropriate due to its relative low sorption capacity. To improve phosphate sorption capacity, laterite can be activated with methods such as thermal treatment [31], alkali treatment [14], ultrasonication [32], and so on. To facilitate the practical application of laterite, thermal treatment should be the most convenient one among the activation methods mentioned above [33].

Herein, the objectives of this study are to (1) optimize the preparation conditions of activated laterite (AL), (2) examine the phosphate adsorption performance of raw laterite (RL) and AL by batch studies, and (3) investigate the feasibility of the column adsorption of phosphate from aqueous solutions.

2. Materials and methods

2.1. Materials

Laterite was taken from a mountain in Dali Bai Autonomous Prefecture, Yunnan Province. Before experiments were performed, the laterite was first dried at 105℃ for 24 h. Then, the dried laterite samples were crushed in a mortar and sieved through a 40 mesh sieve.

2.2. Heat activation of laterite

Batches of dry sample placed in porcelain dishes were heated at various temperatures (300, 500, 700, and 900℃) for various time (0.5, 1, 2, and 3 h) in a muffle furnace. At the end of the treatment, the powder was ground in a mortar and sieved through a 40 mesh sieve again.

2.3. Performance of laterite

Adsorption studies were carried out by shaking (120 rpm) 40 ml of 5.0–30.0 mg/L phosphate (KH_2PO_4, calculated as P) solution with 1.0–5.0 g/L dosage in the bottles for 24 h at 25℃. After equilibrium, the samples were filtered through 0.45 μm syringe filter paper and analyzed for the adsorption efficiency. The removal efficiency (*E*, %) and adsorption capability (Q_e, mg/g) of phosphate on adsorbent were calculated by Eqs. (1) and (2),

$$E = \frac{(C_0 - C_e)}{C_e} \times 100 \tag{1}$$

$$Q_e = \frac{(C_0 - C_e)V}{m} \tag{2}$$

where C_0 and C_e (mg/L) are the initial and equilibrium liquid phase phosphate concentrations, respectively; *V* (L) is the volume of the solution and *m* (g) is the mass of the adsorbent.

The solution pH was adjusted by HCl (0.1 M) or NaOH (0.1 M) solutions, and Na_2SO_4, NaCl, NaF, or $NaNO_3$ solutions were added as the sources of the competing anions when necessary.

As for the kinetic experiments, a fixed amount of adsorbent (1.5 g) was introduced to 300 mL of phosphate solutions (initial concentration: 30.0 mg P/L) in flasks. The flasks were shaken at 120 rpm. The equilibrium adsorption capacity was evaluated on the basis of a mass balance between the initial and final phosphate concentrations.

The concentrations of the phosphate solutions were determined by the ascorbic acid method [22], measuring the absorbance at 700 nm with the UV–Vis spectrophotometer (Model 721, Shanghai Metash Instruments Co., Ltd, China) in liquid cuvette configuration with de-ionized water as reference.

2.4. Column adsorption of laterite

The column adsorption of laterite was performed using a transparent glass column of 1.2 cm inner diameter and 3.0 cm high fitted with laterite (2.5 g). The feed liquid, containing different phosphate concentrations (5.0, 10.0, and 15.0 mg P/L), was passed through the column at various flow rates of 20.0, 25.0, and 30.0 mL/min by peristaltic water pumps. 5 mL effluent liquid was taken out at 10 min intervals to analyze the phosphate concentration.

2.5. Data analysis

2.5.1. Adsorption isotherm equation

The isotherm data were analyzed by Langmuir (Eq. (3)) and Freundlich (Eq. (4)) equations which can be expressed mathematically as follows:

$$\frac{C_e}{q_e} = \frac{C_e}{q_{\max}} + \frac{1}{K_L q_{\max}} \tag{3}$$

$$\ln q_e = \ln K_f + \frac{\ln C_e}{n} \tag{4}$$

where C_e is the equilibrium concentration of phosphate in solution (mg/L); q_e is the correspondent uptake capacity of the adsorbent (mg/g); $q_{\max}$ is the theoretical maximum phosphate adsorption capacity (mg/g) and K_L is the affinity constant (L/mg); K_f (mg/g) and n are Freundlich constants.

2.5.2. Adsorption kinetics

To evaluate the adsorption kinetic process, the phosphate adsorption kinetic data were fitted by pseudo-first- and second-order models. The kinetic equations for these models are as follows [34,35],

$$\log(q_e - q_t) = \log q_e - \frac{k_1 t}{2.303} \tag{5}$$

$$\frac{t}{q_t} = \frac{1}{k_2 q_e^2} + \frac{t}{q_e} \tag{6}$$

where q_e (mg/g) is the equilibrium adsorption capacity, q_t (mg/g) is the adsorption capacity of a moment (t); k_1 (min^{-1}) is the pseudo-first-order reaction kinetics constant; k_2 (mg/g min) is quasi-second-order kinetic constants.

3. Results and discussion

3.1. Effect of heat treatment of laterite on the removal of phosphate

The laterite samples were activated with heat, which resulted in different efficiency of phosphate removal (Fig. 1).

It can be seen from Fig. 1(a), with the increasing of temperature, the adsorption capacity increases, the phosphate removal by the laterite sample calcined at 700℃ for 2 h (AL) achieves 1.83 mg/g, which is higher than those of laterite samples heated at other temperatures and close to that of 900℃. To reduce consumption of energy, 700℃ was chose for following experiment. This mainly was as results of metal form transferred to metal oxide (on which there are much more adsorption sites) and the mass loss (which has no adsorption sites) with the laterite being heated [28].

The heating time also influences the heat activation capability. For example, at 700℃, the activation of laterite with heat was accomplished in the first 2 h. After that, the removal did not increase with the treatment time as shown in Fig. 1(b). During the calcination, the surface area of the laterite might enlarge gradually, as the expulsion of water leads to the development of porosity [28]. The phosphate removal was efficient comparatively when the laterite sample was calcined at 700℃ and then became a little less efficient as temperatures increased or time was prolonged [28]. This is due to the decomposition of some hydroxyl groups, calcite, and the sintering shrinkage of laterite when it is calcined [36].

3.2. Effects of initial P concentration on adsorption capacity and adsorption isotherms

At room temperature, 5.0 g/L dosage of RL and AL, as adsorbents, was added in solutions with different initial phosphorus concentration (5.0, 10.0, 20.0, 25.0, and 30.0 mg P/L) to react for 24 h. Representative plots of adsorption isotherms, q_e vs. C_e for RL and AL, were described in Fig. 2(a). It is seen that q_e increased sharply at low equilibrium concentrations, whereas at higher values of C_e, the increase in q_e was gradual, meaning that maximum adsorption capacity was brought about at high phosphate concentration. The adsorption effect of the high-temperature activation of the laterite is better than the RL, as expected and discussed in Section 3.1 [28,36]. The equilibrium data were analyzed using the Langmuir and Freundlich adsorption isotherms. The results were shown in Fig. 2(b) and (c).

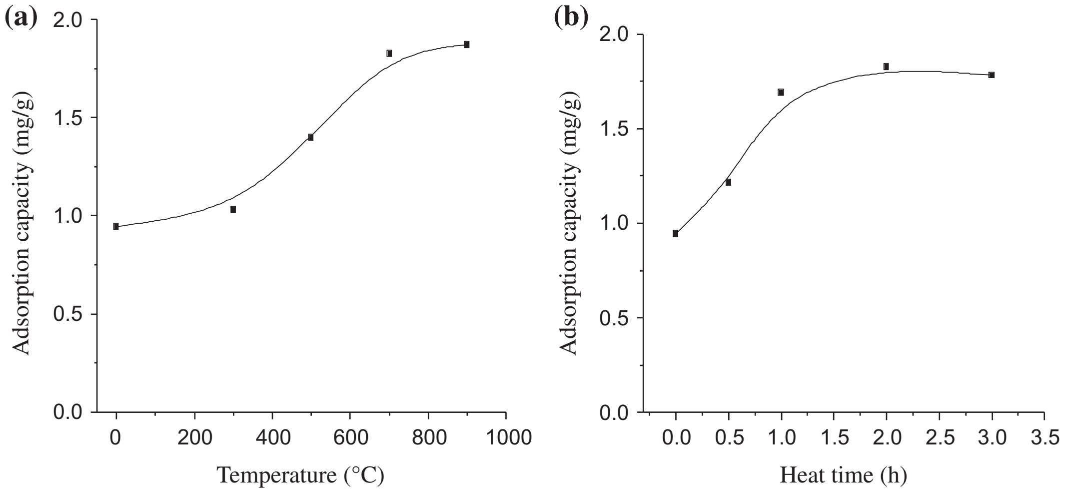

Fig. 1. Effect of heat temperature ((a) heat time: 2 h) and time ((b) heat temperature: 700℃).

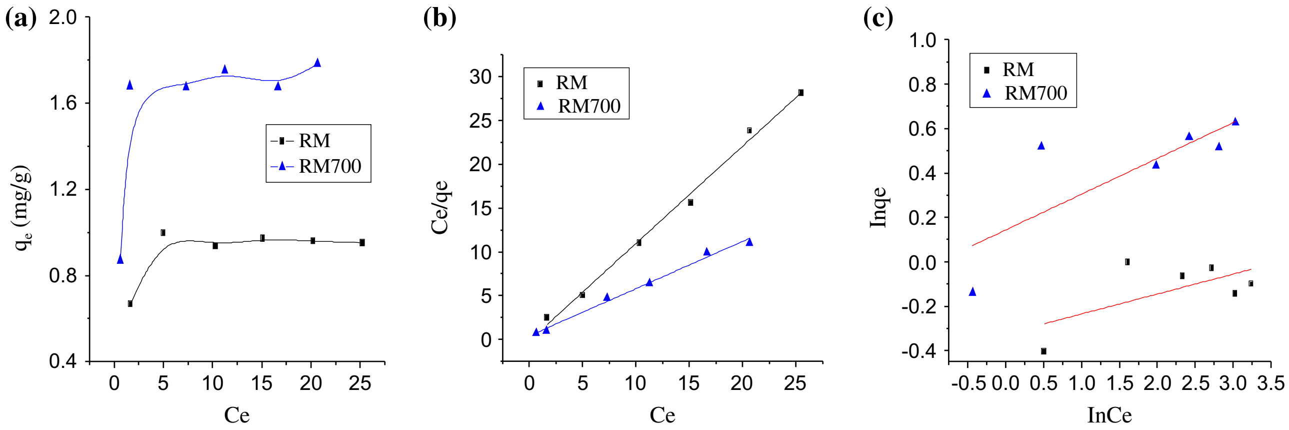

Fig. 2. (a) Adsorption isotherm of phosphate by ACF-NanoHFO, (b) Linear Langmuir adsorption isotherms, and (c) Freundlich adsorption isotherms.

The adsorption parameters and regression coefficients (R^2 values) presented in Table 1 indicated that the adsorption equilibrium data over the concentration range used in this investigation fitted better the Langmuir model than the Freundlich model. The maximum adsorption capacity of RL and AL was calculated to be 0.90 and 1.86 mg/g, respectively, indicating the adsorption process occurs homogeneously which means the adsorption might be chemisorptions [37].

3.3. The effect of reaction time and kinetics model of adsorption

RL and AL were added in 30.0 mg P/L solution with the dosage of 5.0 g/L for (2, 4, 8, 16, and 24 h) at room temperature, the results are shown in Fig. 3(a).

Adsorption kinetic experiments were conducted to determine the rate of phosphate adsorption on the RL and AL. Fig. 3(a) shows that with the reaction time increasing, the adsorption capacity increases gradually until it reaches equilibrium. The changes in capacity of the two sorbents exhibited the same trend. Within

Table 1
Langmuir and Freundlich isotherm constants

Sample	Langmuir isotherm model			Freundlich isotherm model		
	R^2	Q_0 (mg/g)	K_L (L/mg)	R^2	n	K_F (mg/g)
AL	0.993	0.90	−7.35	0.245	11.14	0.72
AL	0.989	1.86	1.27	0.548	6.20	1.15

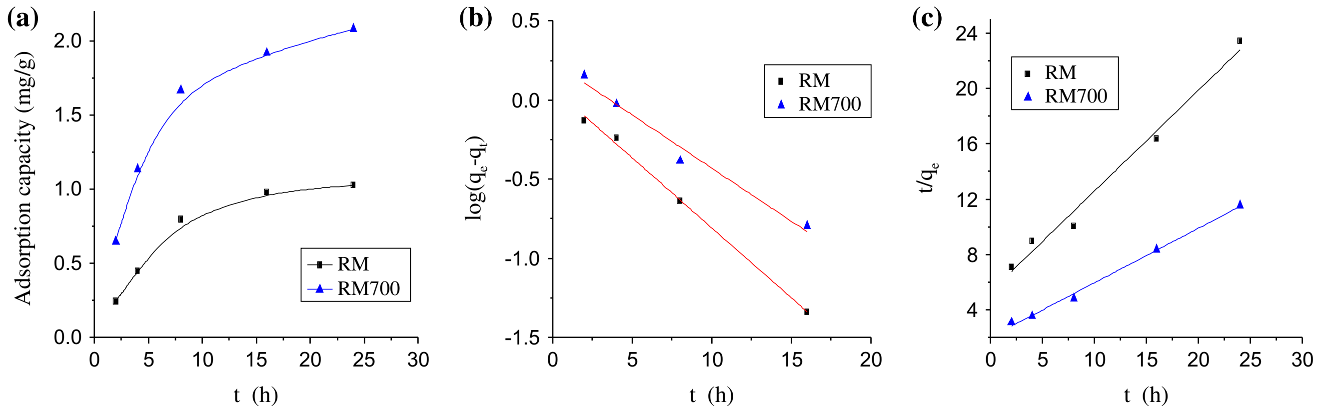

Fig. 3. (a) Effect of contact time and initial concentration on the adsorption amount of phosphate onto RL and AL, (b) pseudo-first-order plots for adsorption of phosphate on the adsorbent, and (c) pseudo-second-order plots for adsorption of phosphate on the adsorbent.

the first 10 h, the adsorption amount increased quickly and then became stable until the adsorption became the equilibrium.

To evaluate the adsorption kinetic process, the phosphate adsorption kinetic data were fitted by pseudo-first- and second-order models, which were shown in Fig. 3(b) and (c). The kinetic parameters of phosphate in the laterite and AL were presented in Table 2.

According to Table 2, it can be seen that the R^2 of the second order kinetic model is superior to the first-order kinetic model. Therefore, the pseudo-second-order model is more suitable for the kinetic behavior of phosphate in the RL and AL as compared with the pseudo-first-order model, which suggests that the adsorption process might be chemisorptions [37]. This possibly happens because phosphate exchange with hydroxyl on the surface of metal oxide to form hydrogen phosphate in water solution with pH of around 7.0, meaning that there is special affinity between phosphate and the adsorbent with good adsorption effect but maybe hard regeneration. It should be noted that the adsorption capacity and rate is always higher than laterite during the adsorption process.

Table 2
Kinetic parameters for phosphate adsorption on RL and AL

Simple	First-order kinetics			Second-order kinetics		
	k_1 (min^{-1})	q_e (cal) (mg/g)	R^2	k_2 (g/(mg min))	q_e (cal) (mg/g)	R^2
RL	0.203	0.84	0.996	0.101	1.37	0.981
AL	0.155	0.57	0.967	0.078	2.54	0.994

3.4. The effect of dosage

The effect of adsorbent dosage on the percent removal of phosphate and adsorption capacity of adsorbent at various initial phosphate concentrations is shown in Fig. 4.

The experimental results revealed that phosphate removal efficiency increased with the adsorbent dosage from 1.0 to 5.0 g/L (Fig. 4(a)) as well as the adsorption capacity of adsorbent declined gradually. As expected, the equilibrium concentration decreased with increasing adsorbent doses for a given initial phosphate concentration, because for a fixed initial solute concentration, increasing adsorbent dose provided a greater surface area or more adsorption sites [38]. But the diffusion resistance of phosphate in congregated metal oxides particles might cause the decline of adsorption capacity. The two adsorbents had similar trends because of both decline of adsorption capacity with high dose.

3.5. The effect of initial pH

The phosphate removal by RL and AL was shown in Fig. 5(a) at pH 2, 4, 6, 8, 10, and 12 when the initial phosphate concentration was 30.0 mg/L, and the pH of the solution was also determined after the phosphate removal (Fig. 5(b)).

As can be seen from Fig. 5(a), pH had important influence on phosphate removal efficiency of the two adsorbents.

When the laterite was added into a solution, there exists such surface hydrolysis reactions depending on pH:

$$\equiv \mathrm{SOH} + \mathrm{H}^+ === \equiv \mathrm{SOH}_2^+ \tag{7}$$

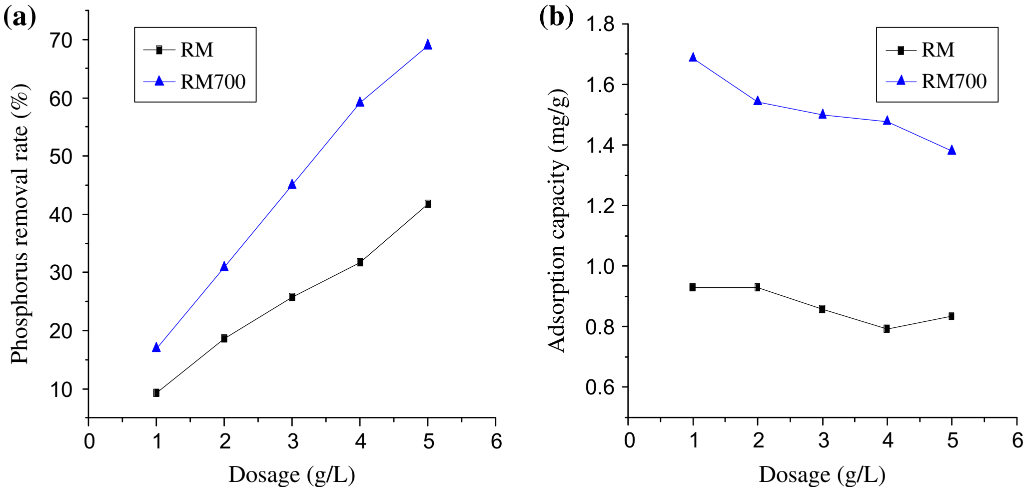

Fig. 4. Effect of adsorbent dosage on phosphate removal rate and adsorption capacity: 10.0 mg P/L solution for 24 h.

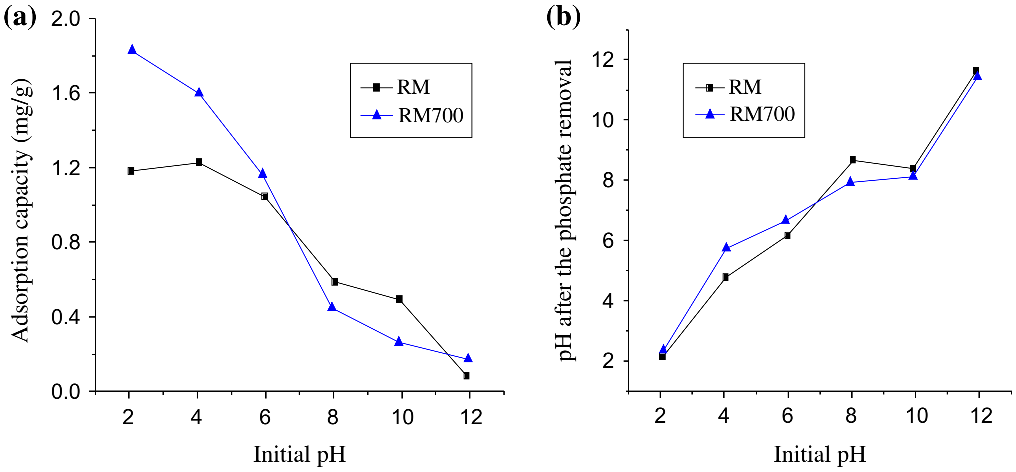

Fig. 5. (a) Effect of solution pH on the adsorption capacity, (b) pH of the solution after the phosphate removal.

$$\equiv \mathrm{SOH} === \equiv \mathrm{SO}^{-} + \mathrm{H}^{+} \qquad (8)$$

In acidic conditions for pH 2–7, the surface of adsorbent with a strong positive charge by the protonation process on metal active site with the reaction (Eq. (7)), the dominant species were $H_2PO_4^-$ and HPO_4^{2-} which readily absorbed by the active on the adsorbent by electrostatic interactions. Meanwhile, the ion exchange might occur by the following reaction, $\equiv MOH + H_2PO_4^- === \equiv MH_2PO_4^- + OH^-$; $\equiv MOH + HPO_4^{2-} === \equiv M_2HPO_4^{2-} + 2OH^-$.

The higher pH not only causes the adsorbent surface to carry more negative charges (Eq. (8)), but also leads to a high concentration of hydroxide groups [33]. Therefore, there might also be increased competition between negatively charged phosphate species and hydroxide groups on more negatively charged adsorbent surface sites to cause the lower adsorption of phosphate at higher pH.

At first, the pH after the phosphate removal was slightly higher than the initial pH, but became lower at the higher pH, which can be observed in Fig. 5(b). This may be due to that the ion exchange reaction between phosphate ions and the hydroxide ions with different exchange amounts at different pH values [39]. The release of OH^- would lead to the increase in final pH, and then with the increasing of pH, the active sits might form stable hydroxides by the competition between phosphate species and hydroxide groups, some hydroxide groups were consumed.

3.6. Competing effect of co-existing anions

Phosphate adsorption on RL and AL was separately investigated in the presence of following

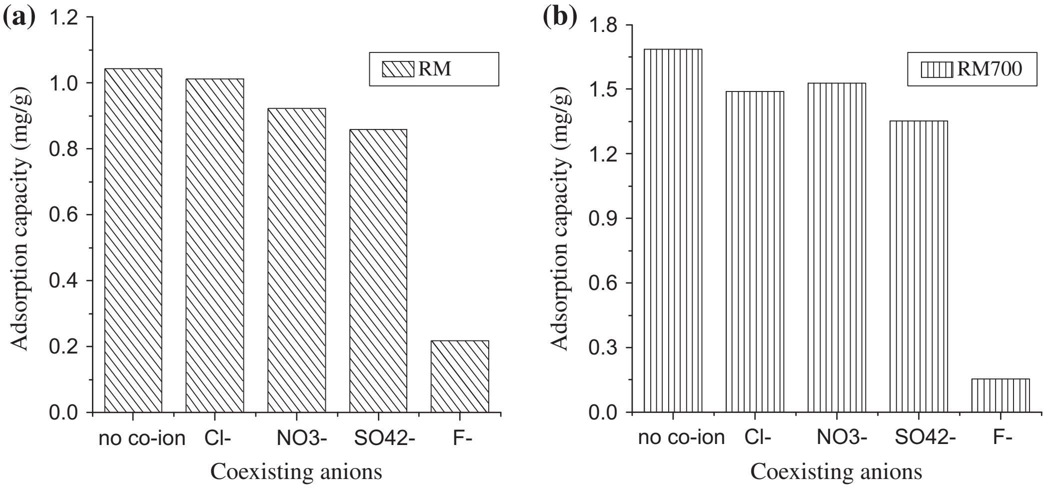

Fig. 6. Effect of coexisting ions on the phosphate adsorption.

competing anions: F^-, Cl^-, NO_3^-, and SO_4^{2-} [40]. As shown in Fig. 6, a decrease in phosphate removal was observed when the concentration of competitive ions was 50.0 mg/L when the initial phosphate concentration was 10.0 mg/L. The four competing anions had different adverse effect on phosphate removal. The inhibition on phosphate adsorption of RL and AL follows the order: $F^- > SO_4^{2-} > NO_3^- > Cl^-$ and $F^- > SO_4^{2-} > Cl^- > NO_3^-$, respectively. Among the four anions, F^- had largest impact on the adsorption of phosphate for both adsorbents. An ion exchange reaction may be proposed as a mechanism for phosphate adsorption in this material. Thus, the decrease in the adsorption capacity can be explained on the basis of ion exchange mechanism where fluoride ion possessed the highest affinity for the adsorbent material and competes most effectively against phosphate adsorption [33,39]. The order of the effect of the other anions on the phosphate adsorption may also be related to affinity of the anions toward the adsorbent.

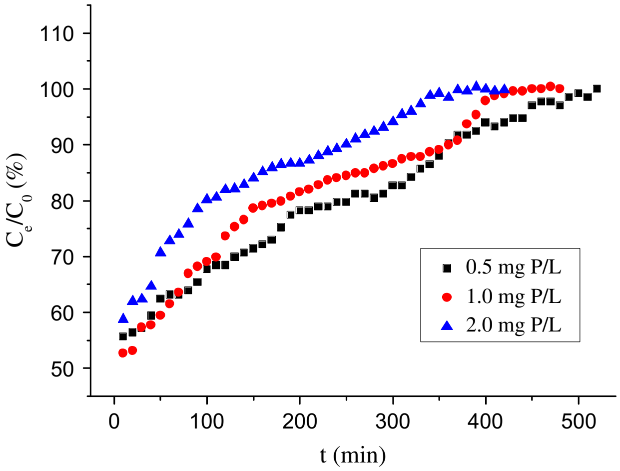

Fig. 7. Flow rate of 20.0 mL/min with different initial phosphorus concentration of phosphorus removal.

3.7. The column adsorption of AL

The adsorption columns were operated with different initial phosphorus concentration (0.5, 1.0, and 2.0 mg P/L) until no further phosphate removal was observed. The breakthrough curve for a column was determined by plotting the ratio of the C_e/C_0 (C_e and C_0 are the phosphate concentration of effluent and influent, respectively) against the time. The experimental results were presented in Fig. 7.

As expected, the first phase of the adsorption, phosphate concentration of the effluent increased slowly, because there were sufficient adsorption sites for phosphate adsorption on the adsorbent, making export concentration low and the adsorption point decrease with time going by. At last, the phosphate concentration of the effluent slowly closed to the initial concentration, meaning that the adsorbent was saturated. From Fig. 7 and it was found that the lower the phosphate concentration of the influent was, the longer time the column worked. This might be explained by that the concentration gradient was enhanced or mass transfer resistance force decreased at high phosphate concentration [41], which led to high adsorption rate to make the active sites more quickly saturated in the column.

4. Conclusions

The uptake of phosphate by RL and AL was compared in this study, and the factors influencing the laterite activation were investigated. The phosphate sorption capacity can be enhanced by the activation. In the heat activation process, the optimum activation was the laterite calcined at 700℃ for 2 h. The pH has a significant effect on phosphate sorption. The maximum phosphate adsorption is achieved within the pH range of 2–6. The adsorption of phosphate by RL and AL in batch systems can be described by the Langmuir isotherm, and the adsorption capacity (cal) was 0.90 mg/g and 1.86 mg/g, respectively. In Kinetic experiments, the data fit well to the pseudo-second-order model, which suggests that the adsorption process might be chemisorptions. The column adsorption experiments showed that high phosphate concentration leads to high adsorption rate, the adsorbent saturated faster. All the results illustrate that the laterite should be an ideal material for transformation for phosphate adsorption, such as granulation.

Acknowledgements

This project is financially supported by National Science Foundation of China No. 21207085 and Shanghai Leading Academic Discipline Project No. S30109. We also thank the alliance program (Project No. LM2011057) funded by Shanghai Promotion Association of Tech-transfer (SPAT), Shanghai Education Development Foundation (SEDF) and Shanghai Promotion of Tech-transfer Foundation (SPTF) for financial supports.

References

[1] J.W. Choi, S.Y. Lee, K.Y. Park, K.B. Lee, D.J. Kim, S.H. Lee, Investigation of phosphorous removal from wastewater through ion exchange of mesostructure based on inorganic material, Desalination 266 (2011) 281–285.

[2] Y. Song, P. Yuan, B. Zheng, J. Peng, F. Yuan, Y. Gao, Nutrients removal and recovery by crystallization of magnesium ammonium phosphate from synthetic swine wastewater, Chemosphere 69 (2007) 319–324.

[3] D. Mulkerrins, A.D.W. Dobson, E. Colleran, Parameters affecting biological phosphate removal from wastewaters, Environ. Int. 30 (2004) 249–259.

[4] J.G. Vieira, A.G. da Silva Manetti, E. Jacob-Lopes, M.I. Queiroz, Uptake of phosphorus from dairy wastewater by heterotrophic cultures of cyanobacteria, Desalin. Water Treat. 40 (2012) 224–230.

[5] L.J. Sherwood, R.G. Qualls, Stability of phosphorus within a wetland soil following ferric chloride treatment to control eutrophication, Environ. Sci. Technol. 35 (2001) 4126–4131.

[6] K.S. Narasiah, C. Morasse, J. Lemay, Phosphorus removal from aerated lagoons using alum, ferric chloride and lime, Water Qual. Res. J. Can. 29 (1994) 1–18.

[7] J. Paul Chen, M.L. Chua, B. Zhang, Effects of competitive ions, humic acid, and pH on removal of ammonium and phosphorous from the synthetic industrial effluent by ion exchange resins, Waste Manage. 22 (2002) 711–719.

[8] I. de Vicente, P. Huang, F.Ø. Andersen, H.S. Jensen, Phosphate adsorption by fresh and aged aluminum hydroxide. Consequences for lake restoration, Environ. Sci. Technol. 42 (2008) 6650–6655.

[9] M.S. Onyango, D. Kuchar, M. Kubota, H. Matsuda, Adsorptive removal of phosphate ions from aqueous solution using synthetic zeolite, Ind. Eng. Chem. Res. 46 (2007) 894–900.

[10] M. Albertsen, L.B.S. Hansen, A.M. Saunders, P.H. Nielsen, K. L. Nielsen, A metagenome of a full-scale microbial community carrying out enhanced biological phosphorus removal, ISME J. 6 (2012) 1094–1106.

[11] V. Bucci, N. Majed, F.L. Hellweger, A.Z. Gu, Heterogeneity of intracellular polymer storage states in enhanced biological phosphorus removal (EBPR)—observation and modeling, Environ. Sci. Technol. 46 (2012) 3244–3252.

[12] N. Majed, T. Chernenko, M. Diem, A.Z. Gu, Identification of functionally relevant populations in enhanced biological phosphorus removal processes based on intracellular polymers profiles and insights into the metabolic diversity and heterogeneity, Environ. Sci. Technol. 46 (2012) 5010–5017.

[13] H.S. Altundogan, F. Tumen, Removal of phosphates from aqueous solutions by using bauxite II: The activation study, J. Chem. Technol. Biotechnol. 78 (2003) 824–833.

[14] C.Z. Yu, J. Yang, L.A. Zhou, L.Z. Zhao, H.W. Zhang, J.N. Yin, G.F. Wei, K. Qian, Y.H. Wang, A designed nanoporous material for phosphate removal with high efficiency, J. Mater. Chem. 21 (2011) 2489–2494.

[15] E. Galarneau, R. Gehr, Phosphorus removal from wastewaters: Experimental and theoretical support for alternative mechanisms, Water Res. 31 (1997) 328–338.

[16] S.J. Shiao, K. Akashi, Phosphate removal from aqueous solution from activated red mud, J. Water Pollut. Control Fed. 49 (1977) 280–285.

[17] J. Pradhan, J. Das, S. Das, R.S. Thakur, Adsorption of phosphate from aqueous solution using activated red mud, J. Colloid Interface Sci. 204 (1998) 169–172.

[18] E. Oguz, Sorption of phosphate from solid/liquid interface by fly ash, Colloids Surf., A 262 (2005) 113–117.

[19] N.M. Agyei, C.A. Strydom, J.H. Potgieter, An investigation of phosphate ion adsorption from aqueous solution by fly ash and slag, Cem. Concrete Res. 30 (2000) 823–826.

[20] N.M. Agyei, C.A. Strydom, J.H. Potgieter, The removal of phosphate ions from aqueous solution by fly ash, slag, ordinary Portland cement and related blends, Cem. Concrete Res. 32 (2002) 1889–1897.

[21] A. Tor, N. Danaoglu, G. Arslan, Y. Cengeloglu, Removal of fluoride from water by using granular red mud: Batch and column studies, J. Hazard. Mater. 164 (2009) 271–278.

[22] G. Cappai, G. De Gioannis, A. Muntoni, D. Spiga, J.J.P. Zijlstra, Combined use of a transformed red mud reactive barrier and electrokinetics for remediation of Cr/As contaminated soil, Chemosphere 86 (2012) 400–408.

[23] R.C. Sahu, R. Patel, B.C. Ray, Adsorption of Zn(II) on activated red mud: Neutralized by CO2, Desalination 266 (2011) 93–97.

[24] E. Lopez, B. Soto, M. Arias, A. Núņez, D. Rubinos, M.T. Barral, Adsorbent properties of red mud and its use for wastewater treatment, Water Res. 32 (1998) 1314–1322.

[25] J. Pradhan, S.N. Das, R.S. Thakur, Adsorption of hexavalent chromium from aqueous solution by using activated red mud, J. Colloid Interface Sci. 217 (1999) 137–141.

[26] F. Ni, X. Peng, Y. Zhao, J. He, Y. Li, Z. Luan, Preparation of coagulant from red mud and semi-product of polyaluminum chloride for removal of phosphate from water, Desalin. Water Treat. 40 (2012) 153–158.

[27] W. Huang, S. Wang, Z. Zhu, L. Li, X. Yao, V. Rudolph, F. Haghseresht, Phosphate removal from wastewater using red mud, J. Hazard. Mater. 158 (2008) 35–42.

[28] Y. Li, C. Liu, Z. Luan, X. Peng, C. Zhu, Z. Chen, Z. Zhang, J. Fan, Z. Jia, Phosphate removal from aqueous solutions using raw and activated red mud and fly ash, J. Hazard. Mater. 137 (2006) 374–383.

[29] H.J. Choi, S.M. Lee, Effect of particle size distribution in wastewater on the performance of nutrient removal process, Desalin. Water Treat. 46 (2012) 227–233.

[30] L. Zhang, S. Hong, J. He, F. Gan, Y.S. Ho, Adsorption characteristic studies of phosphorus onto laterite, Desalin. Water Treat. 25 (2011) 98–105.

[31] J.Y. Liu, L. Zhang, L.H. Wan, N. Chang, C. Duan, Q. Zhou, X.L. Li, X.Z. Wang, Removal of phosphate from water by activated carbon fiber loaded with lanthanum oxide, J. Hazard. Mater. 190 (2011) 848–855.

[32] L. Zhang, Q. Zhou, J. Liu, N. Chang, L. Wan, J. Chen, Phosphate adsorption on lanthanum hydroxide-doped activated carbon fiber, Chem. Eng. J. 185–186 (2012) 160–167.

[33] J. Liu, L. Wan, L. Zhang, Q. Zhou, Effect of pH, ionic strength, and temperature on the phosphate adsorption onto lanthanum-doped activated carbon fiber, J. Colloid Interface Sci. 364 (2011) 490–496.

[34] S. Lagergren, Zur theorie der sogenannten adsorption geloster stoffe [Theory of the so-called absorption of dissolved substances], Kungliga Svenska Vetenskapsakademiens, Handlingar 24 (1898) 1–39.

[35] G. Blanchard, M. Maunaye, G. Martin, Removal of heavy metals from waters by means of natural zeolites, Water Res. 18 (1984) 1501–1507.

[36] C.-J. Liu, Y.-Z. Li, Z.-K. Luan, Z.-Y. Chen, Z.-G. Zhang, Z.-P. Jia, Adsorption removal of phosphate from aqueous solution by active red mud, J. Environ. Sci. 19 (2007) 1166–1170.

[37] J. Yang, L. Zhou, L. Zhao, H. Zhang, J. Yin, G. Wei, K. Qian, Y. Wang, C. Yu, A designed nanoporous material for phosphate removal with high efficiency, J. Mater. Chem. 21 (2011) 2489–2494.

[38] S. Rengaraj, S.H. Moon, Kinetics of adsorption of Co (II) removal from water and wastewater by ion exchange resins, Water Res. 36 (2002) 1783–1793.

[39] Y. Xue, H. Hou, S. Zhu, Characteristics and mechanisms of phosphate adsorption onto basic oxygen furnace slag, J. Hazard. Mater. 162 (2009) 973–980.

[40] Q. Zhou, X. Wang, J. Liu, L. Zhang, Phosphorus removal from wastewater using nano-particulates of hydrated ferric oxide doped activated carbon fiber prepared by Sol–Gel method, Chem. Eng. J. 200–202 (2012) 619–626.

[41] L. Zhang, J. Liu, L. Wan, Q. Zhou, X. Wang, Batch and fixed-bed column performance of phosphate adsorption by lanthanum-doped activated carbon fiber, Water Air Soil Pollut. 223 (2012) 1–10.